# Improved filtration properties of hydroentangled PTFE/PPS fabric filters caused by fibrillation

Zhang Nan[1], Jin Xiang-yu[1,a], Huang Chen[1] & Ke Qin-fei[2,b]

[1]Engineering Research Center of Technical Textiles, Donghua University, Shanghai 201600, China

[2]Shanghai Normal University, Shanghai 200234, China

The effect of specific energy on fibre diameter of polytetrafluoro ethylene / polyphenylene sulfide (PTFE/PPS) blended fabrics has been studied. The influence of blend ratio and bonding process on air permeability, mean flow pore size and filtration properties are also studied. The results show that fibrillation of PTFE fibres could be induced and regulated by high-energy water jets. With the increase of fibrillated PTFE fibres, the mean pore size and air permeability of the fabric decrease, leading to an increased filtration properties.

**Keywords**: Blended fabrics, Fibrillation, Filtration properties, Hydroentanglement, PTFE fibres, PTFE/PPS blend

## 1 Introduction

With the economic growth in developing regions, air pollution has become one of the major subjects and has brought harmful effects to our daily life. One of the major causes of air pollution is the industrial emission of particulate matter. The conventional devices for controlling particulate matter emission include cyclones, wet scrubbers, electrostatic precipitators, and baghouses; among them baghouses have attracted intensive attention, due to their high dust-collection efficiency (over 99%)[1]. Baghouse made of polyphenylene sulfide (PPS) fibres are widely used in harsh environment because of its high melting point and good resistance of chemical materials. However, the main disadvantage of PPS staple fibres was the weak resistance of oxidation. Winyu *et al.*[2,3] studied the effect of NO and $O_2$ on the degradation of PPS fabric

mechanical properties. In order to overcome these drawbacks, considerable efforts have been made, including chemical treatment such as coating or impregnation with PTFE emulsion or resin, blending with other high performance fibres such as glass fibres, PI fibres and PTFE fibres[4-6]

Blending different types of fibres is a simple and effective way to obtain specific combination of physical

Corresponding authors.
[a]E-mail: Jinxy@dhu.edu.cn
[b]E-mail: kqf@dhu.edhu.cn

properties. Currently, a large number of commercial bag filters has been studied which is composed of two different fibres to achieve a balance of cost and properties. Mukhopadhyay[7] suggested that 100% polyimide (P84) bag filters couldn't be used from technical and economical reasons and combination of P84 with PTFE fibres would be a better choice. Lin *et al.*[1] reported the use of blended needle-punched fabrics as bag filters. However, to the best of our knowledge no study has been reported on the effect of blend ratio of PPS and other high performance fibres on the air permeability and filtration properties of fabric filters to be used as bag filters.

Because of the excellent thermal and chemical stability, PTFE fibres could be blended with PPS fibres to improve the lack of heat and chemical resistance. The bag filters, consisted of PTFE fibres, could be used at the temperature up to 250°C and possessed the ___ and excellent filtration properties. Since PTFE has high-melt viscosity, traditional melt spinning method is not suitable to produce PTFE fibres. Usually the fibres were obtained by blending PTFE fine powder resins with kerosene to form the paste, followed by stretching and sintering. During the extension, the fibrillation could be induced. Li *et al.*[10] studied the model for the variation of submicron structure during the extension and proposed the key point of fabricating the PTFE fibres and the formation of effective and continuous fibrillation. Besides, the PTFE has a tendency to fibrillate, which enabled the formation of fibrils by stretching[11,12].

Normally, bag filters are consolidated by reciprocating barbed needles in needle loom, Yeo *et al.*[13] studied the effect of different processing conditions on the filtration performances of bag filters. Hydroentanglement was another bonding process using high-velocity water jets to entangle the fibres, when the water pressure was high enough, a unique phenomenon of fibrillation could be induced for fibres such as bast and polyacrlonitrile. In this process, a single fibre would be splitted into a few finer fibres, leading to a much smaller fibre diameter. Although Hoeflinge *et al.*[14] studied seven kinds of bag filters consolidated by needle punching or hydroentanglement, the data showed in his research that mean clean gas concentration of hybrid hydroentangled bag filters was lower than that of needle-punched bag filters. There was no systematic study on the effect of specific energy on the structure of hydroentangled bag filters.

Although there were many patents and products about the needle-punched or hydroentangled bag filters used to control particulate emission[15-17], the effect of bonding process and the blend ratio on the properties of PPS and PTFE filters have not been systematically studied. In this paper, we reported the preparation of bag filters formed with four different blend ratios of PTFE and PPS fibres, which are then consolidated by two kinds of bonding processes, viz needle punching and combination of needle punching + hydroentanglement. The influence of specific energy on the average diameter of PTFE fibre has been studied. Under the same specific energy, the air permeability, mean pore size and clean gas concentration of fabrics for the four different blend ratios of fabrics consolidated by different bonding processes are also investigated.

## 2 Materials and Methods

### 2.1 Materials

Polyphenylene sulfide (PPS) fibres were supplied by Toray Industries Inc. Polytetrafluoro ethylene (PTFE) fibres and PTFE woven substrates both were provided by Shanghai JinYou Fluorine Materials Co. Ltd. Characteristics of PPS and PTFE fibres are shown in Table 1.

### 2.2 Sample Preparation

The samples were composed of three layers with PTFE woven fabrics in the middle and the two batts located respectively at the top and bottom of the woven

Table 1 — Characteristics of PPS and PTFE fibres

| Fibre | Length mm | Fineness dtex | Diameter μm | Melting temperature $^0$C |
|---|---|---|---|---|
| PPS | 51 | 1.94[a] | 14.32[b] | 285 |
| PTFE | 51 | 3.50[a] | 31.45[b] | 327 |

[a]Provided by supplier.
[b]Calculated by measuring 500 fibres from SEM images.

fabrics. Then these three layers materials were fed into the needling loom. The feeding speed, stroke frequency, and the number of the passes were adjusted to get a punching density of 800 punches cm$^{-2}$. The Groz-Beckert felting needles with designation of 15×18×40×3 R222 G3037 were used at a fixed depth of penetration (10 mm). After needle punching, some samples were fed into hydroentanglement machine having two injectors. One was for pre-wetting at a low pressure of 30 bar, and the other was used to entangle the web at a high pressure of 240 bar. Schematic illustration of the bonding process is shown in Fig 1.

The PTFE fibres were blended with PPS fibres to fabricate the samples with different PTFE/PPS blend ratios (0:100, 25:75, 50:50 and 75:25). Detailed description of the fabrics is given in Table 2. In order to study the effect of specific energy on the structure and average diameter of PTFE fibres, fabric filters composed of 75% PTFE fibres were fed into the injectors one, two, three and four times respectively to get four different specific energies. The specific energy (E) in Jkg$^{-1}$ applied to the fabric by an injector was calculated according to following equation[18]:

$$E = 6.66 \times 10^4 \frac{C_d d^2 N P^{3/2}}{\sqrt{\rho}WS} \qquad \dots (1)$$

where $C_d$ is the orifice coefficient (assumed 0.7); $d$, the diameter of the jet orifice, $m$ (here $d= 120 \times 10^{-6}$ m); $N$, the number of orifices/m per injector (here $N$=999 orifices/m); $\rho$, the water density, (kg m$^{-3}$); $W$, the basic weight of the web(g m$^{-2}$); and $S$, the line speed (m min$^{-1}$). The total specific energy was calculated according to following equation:

$$E_t = \sum_{i=1}^{p} \sum_{j=1}^{m} E_{ij} \qquad \dots (2)$$

where $E_{ij}$ is the specific energy applied to the fabric by injector; and $j$ ($j$=1,2…$m$), calculated by Eq (1), in the hydroentanglement number of passages $i$ ($i$=1,2,…$p$).
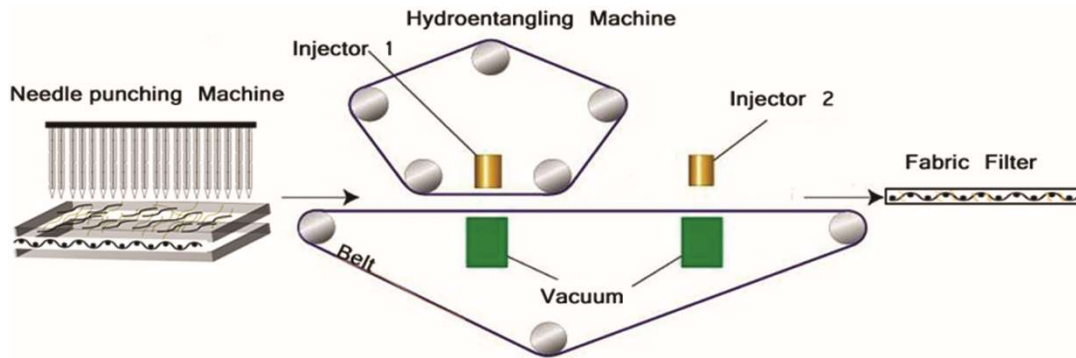
Fig. 1 — Schematic diagram of needle punching and hydroentanglement process

Table 2 — Description of fabrics with different blend ratios and parameters of bonding process

| Sample ID | Bonding process | blend ratio PTFE/PPS | Hydroentanglement number of passages | Specific energy ×10³, kJ kg⁻¹ |
|---|---|---|---|---|
| NH1$_{25}$ | N+H | 75:25 | 1 | 2.17 |
| NH2$_{25}$ | N+H | 75:25 | 2 | 4.25 |
| NH3$_{25}$ | N+H | 75:25 | 3 | 6.33 |
| NH4$_{25}$ | N+H | 75:25 | 4 | 8.41 |
| N$_{25}$ | N | 75:25 | None | – |
| NH4$_{50}$ | N+H | 50:50 | 4 | 8.41 |
| N$_{50}$ | N | 50:50 | None | – |
| NH4$_{75}$ | N+H | 25:75 | 4 | 8.41 |
| N$_{75}$ | N | 25:75 | None | – |
| NH4$_{100}$ | N+H | 0:100 | 4 | 8.41 |
| N$_{100}$ | N | 0:100 | None | – |

N–Needle punching process. H–Hydroentanglement process.

The other three samples with different blend ratios were hydroentangled through injectors four times with a fixed water pressure of 240 bar.

**2.3 Testing Methods**

*2.3.1 Structure and Average Fibre Diameter*

The microstructure of fabrics before and after hydroentanglement were observed by scanning electron microscopy (SEM, TM 300 HITACHI, Japan). Image J software was used to measure the diameters of PTFE fibres from SEM images, and the average fibre diameters were calculated from the measured 500 fibre diameters. Pore size of fabric filters was measured by a capillary flow porometer instrument (CFP-1100-AI, PMI Porous Materials Int., USA). The samples were completely wetted by wetting agent (surface tension was 15.9 dyne cm⁻¹) before pore size test.

The fibre volume fraction ($V_f$, also called solid volume fraction) of blended PTFE/PPS fabrics was calculated from the following equation[19]:

$$V_f = \frac{P_F}{P_f} \qquad \ldots(3)$$

where $P_F$ is the fabric density; and $P_f$, the average fibre density of the blended nonwoven material, which was calculated by the following equation[20]:

$$P_f = \rho_1 s_1 + \rho_2 s_2 \qquad \ldots (4)$$

where $s_1$ & $s_2$ are the weight percentage of PTFE and PPS respectively; $\rho_1$, the density of PTFE ($\rho_1$=2.14 g cm⁻³); and $\rho_2$, the density of PPS ($\rho_2$=1.35 g cm⁻³).

*2.3.2 Air Permeability and Filtration Properties*

Air permeability of fabrics through a given area (20 cm²) was measured according to the ISO 9237:1995; the pressure drop across the fabric test area was set as 200 Pa for industrial fabrics and every test was repeated 10 times at different locations.

The filtration properties for pulse-jet filters were performed using a testing apparatus (Fig. 2) according to VDI 3926:2004, which was used to characterize and evaluate the properties for bag filters after a long-term clogging and cleaning cycles.

The whole test procedure could be divided into 4 phases, namely conditioning, aging, stabilizing and measuring[21]. Going through the whole test procedures,

the residual dust mass and the residual pressure drop of the test filter were investigated. The residual pressure drop is referred to the differential pressure between front and back of the fabric filter after cleaning. The mass of dust penetrating the test filter was collected by absolute filter located at the end of the horizontal tube, then the increased mass of absolute filter was divided by gas volume, thereby the clean-gas concentration could be determined. Here, lower clean-gas concentration equals lower dust mass penetrating the test filter, which indicates the higher filtration efficiency.

## 3 Results and Discussion

### 3.1 Structure and Average Fibre Diameter

Figure 3A shows the SEM image of fabric filters composed of PTFE:PPS (75:25) fibres. These fabrics were consolidated only by needle punching. Figure 3B shows the corresponding fibre diameter distribution. No obvious fibrillation is found on the surface of the PTFE fibres and the inter-fibre voids are found considerable large due to the loose structure. The fibre diameter ranges from 3 μm to 180 μm and the proportion of fibre diameter ranges from 3 μm to 10 μm accounted for a small part( ~20%).

Figures 4 (A-H) show the SEM images of fabric filters consolidated by combination of needle punching and hydroentanglement. Specific energies ($\times 10^3$, kJ kg$^{-1}$) are set as 2.17, 4.25, 6.33, 8.41 respectively. Figures 4 (I-L) show the corresponding fibre diameter distribution. Figures 4 (A-D) show that when high-velocity water jets are applied to fabrics, the surface becomes hairy and the size of inter-fibre voids is reduced, resulting from the more compact structure of
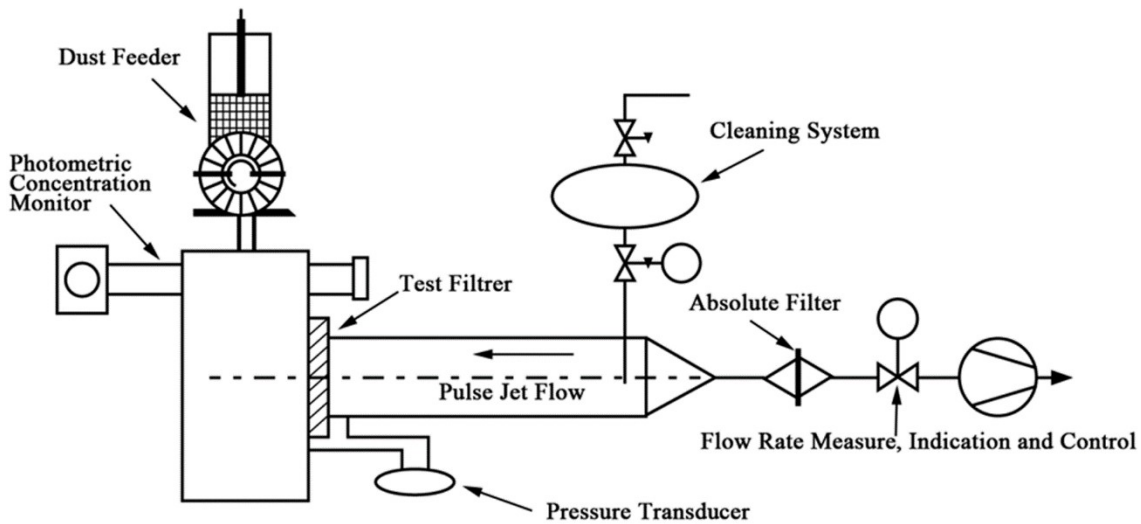


Fig. 2 — Filtration test apparatus according to VDI 3926-2004
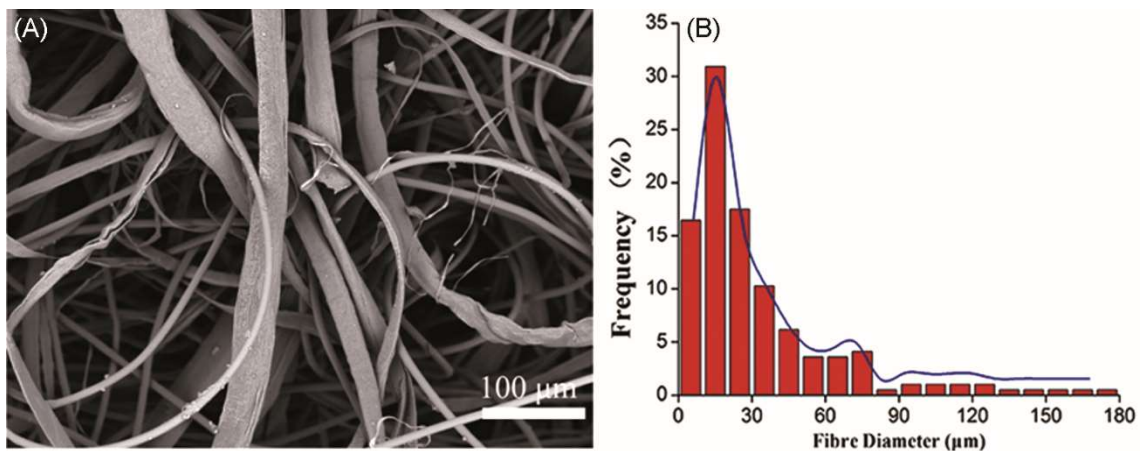


Fig. 3 — Typical SEM images (A), and diameter distribution of 75:25 PTFE:PPS fabric filters (B) only consolidated by needle punching

fabrics and the finer fibres liberated from coarse PTFE fibres. It could be clearly observed from Figs 4 (E-H) that fibrils are generated from the existing PTFE fibres, indicating further splitting of fibres by high-energy water jets; the finest fibre in each figure ranges from 0.2 μm to 0.6 μm. Figures 4 (I-L) show that as the specific energies are increased, the diameter distribution of PTFE fibres becomes narrower, meanwhile the fabrics with highest specific energy has the highest proportion of PTFE fibres ranged between 0.1 μm and 10 μm. The average PTFE fibre diameter of each sample is given below:

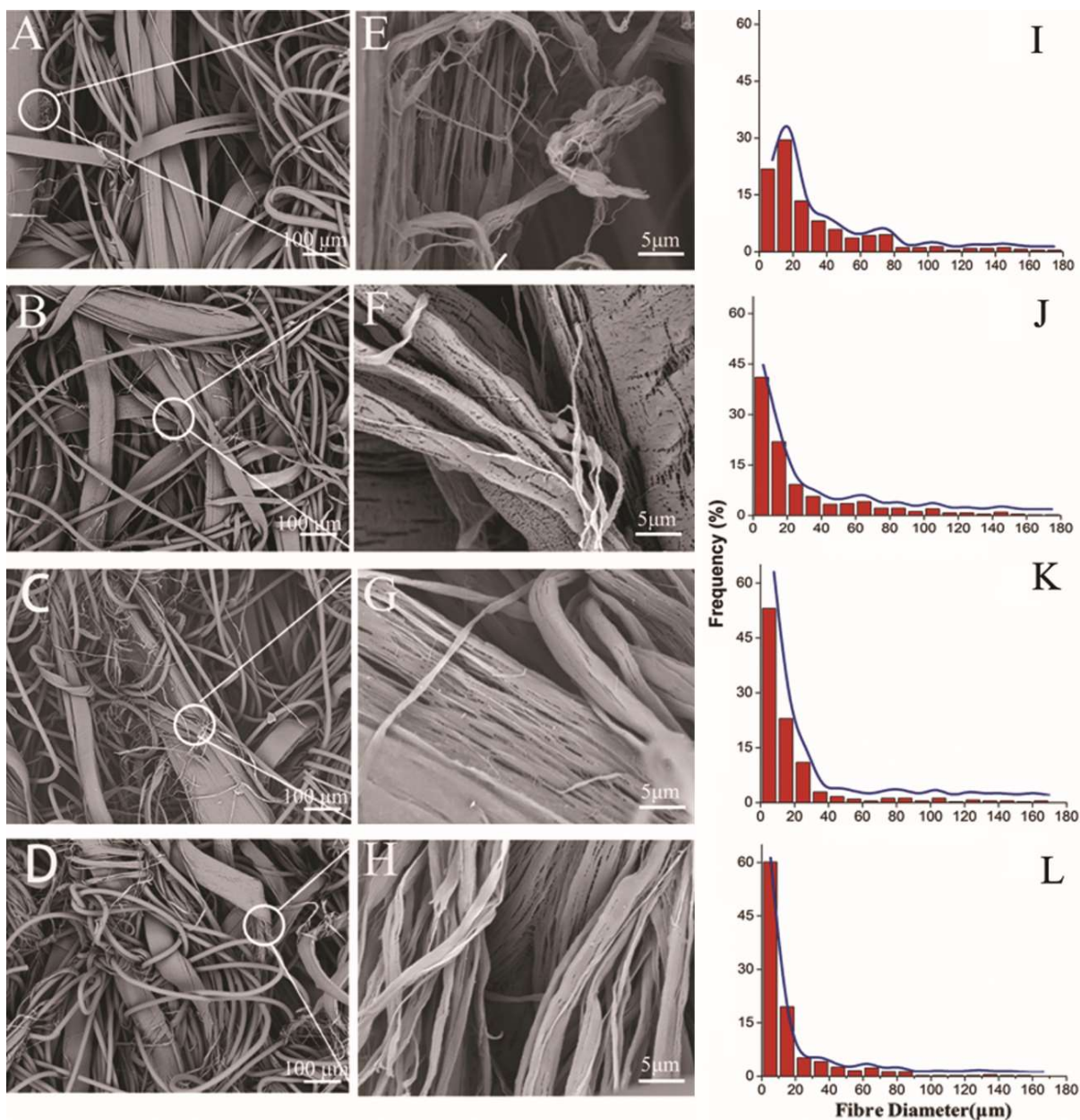| Sample | Avg fibre diam., μm |
|---|---|
| Raw | 31.45 |
| Needle punched | 30.32 |
| Needle punched+ hydroentangled | |
| 2.17×10³, kJ kg⁻¹ | 26.32 |
| 4.25×10³, kJ kg⁻¹ | 20.15 |
| 6.33×10³, kJ kg⁻¹ | 15.72 |
| 8.41×10³, kJ kg⁻¹ | 11.31 |



Fig. 4 — Typical SEM images and diameter distribution of 75:25 PTFE:PPS fabric filters with different specific energies (×10³ kJ kg⁻¹), (A,I) 2.17, (B,J) 4.25, ( C,K) 6.33, and (D,L) 8.41 respectively, and the E, F, G & H are the magnification of white circle in A, B, C & D respectively

As compared to raw material, the average diameter of PTFE fibres is slightly decreased after needle punching, probably due to the fact that the branches split by the ball points and bars of needles. Similar phenomenon is also reported in other study[22], where further splitting is observed during the felting process and the fibre diameter becomes finer. However, an evident decline in average diameter occurs after hydroentanglement, and it decreases with increasing the specific energy. This may be attributed to the reason that PTFE fibres are much easier to be fibrillated[10]. The high energy generated by high-velocity water jets induces such fibrillation of PTFE fibres. As the finer diameter implies better filtration efficiency, the optimal specific energy is chosen as $8.41 \times 10^3$ kJ kg$^{-1}$.

### 3.2 Effect of Blend Ratio and Bonding Process on Air Permeability

Statistical analysis has been done to check whether the air permeability, mean pore size and clean gas concentration are significantly different in terms of blend ratio and bonding process. If the p value is smaller than 0.05, the change in parameter would be significant. The results of variance analysis are shown in Table 3. From this table, two-way ANOVA tests clearly indicate that the blend ratio and the bonding process has strong effects on these properties.

Figure 5(a) shows the air permeability of fabrics composed of four different blend ratios and consolidated by two kinds of bonding processes such as needle punching and combination of needle punching and hydroentanglement with a fixed specific energy of $8.41 \times 10^3$ kJ kg$^{-1}$. In addition, the $V_f$ is added due to its importance and the relation between $V_f$ and blend ratio is shown in Fig. 5(b)[23].

Figure 5(a) shows that for the fabrics consisted of same component, air permeability decreases due to the increased air flow resistance caused by the hydreoentanglement; this decrease is statistically

Table 3 — Analysis of variances for air permeability, mean pore size and clean gas concentration

| Testing properties | Sources of variances | Sums of squares | Degree of freedom | Mean square | *F* value | *P* value |
|---|---|---|---|---|---|---|
| Air permeability | Bonding process | 233782.470 | 1 | 233782.470 | 520.888 | 0.000 |
| | Blend ratio | 10297.903 | 3 | 3432.634 | 7.648 | 0.000 |
| | Interaction | 24602.048 | 3 | 8200.683 | 18.272 | 0.000 |
| | Error | 32314.688 | 72 | 448.815 | | |
| | Total | 467889.450 | 80 | | | |
| Mean pore size | Bonding process | 1247.969 | 1 | 1247.969 | 960.471 | 0.000 |
| | Blend ratio | 14.807 | 3 | 4.936 | 3.799 | 0.031 |
| | Interaction | 54.263 | 3 | 18.088 | 13.921 | 0.000 |
| | Error | 20.789 | 16 | 1.299 | | |
| | Total | 18674.874 | 24 | | | |
| Clean gas concentration | Bonding process | 0.810 | 1 | 0.810 | 1.620E3 | 0.000 |
| | Blend ratio | 0.007 | 3 | 0.002 | 4.583 | 0.038 |
| | Interaction | 0.330 | 3 | 0.110 | | |
| | Error | 0.004 | 8 | | | |
| | Total | 8.576 | 16 | | | |
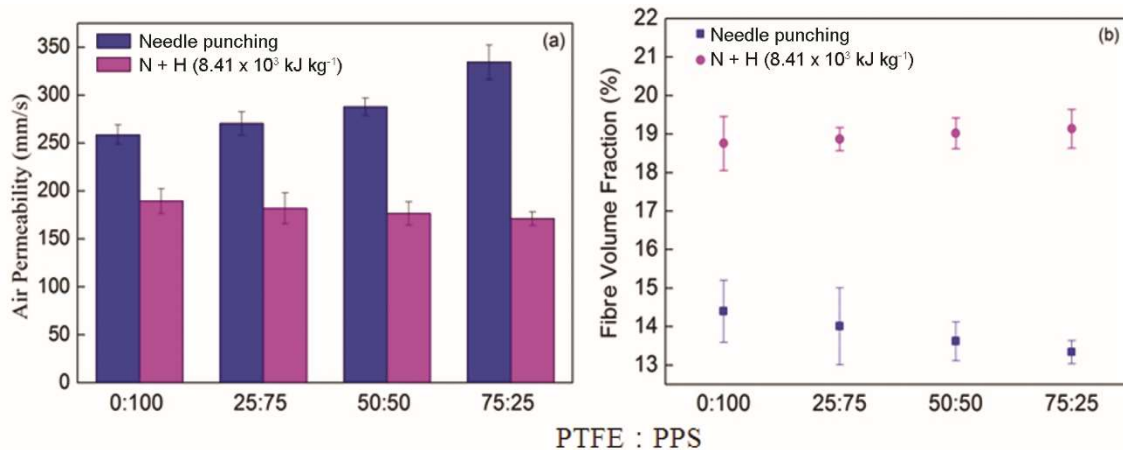


Fig. 5 — (a) Relation of blend ratio and air permeability and (b) relation of blend ratio and fibre volume fraction of hybird fabric filters consolidated by different bonding process (needle punching and composite bonding process with specific energy of $8.41 \times 10^3$ kJ kg$^{-1}$)

important. Because of the high energy applied to the fabric filters, the bonding points are increased and the structure becomes more compacted [Fig. 5(b)][24]. The $V_f$ increases after hydroentanglement, this is found in accordance with other reports that higher $V_f$ leads to lower air permeability[19,25].

Figure 5(a) shows that air permeability(Ap) increases with the increase in PTFE fibres in blend for fabrics consolidated only by needle punching. As both diameter and density of PTFE fibres are larger than those of PPS fibres, there are less PTFE fibres than PPS fibres for identical fabric mass per unit area. Therefore, the total surface area exposed to the air flowing is reduced, leading to an increased air permeability[26]. However, Ap shows a decreased trend with the increased blend ratio of PTFE fibres after the fabrics are hydroentangled. This could be attributed to the decrease in diameter of PTFE fibres. On the other hand, the finer diameter could facilitate more effective entanglement of fibres, which, in turn, produce compact fabrics with higher $V_f$[27].

### 3.3 Effect of Blend Ratio and Bonding Process on Mean Pore Size

Figure 6 shows the relationship of mean flow pore size and blend ratio of the fabrics consolidated by two
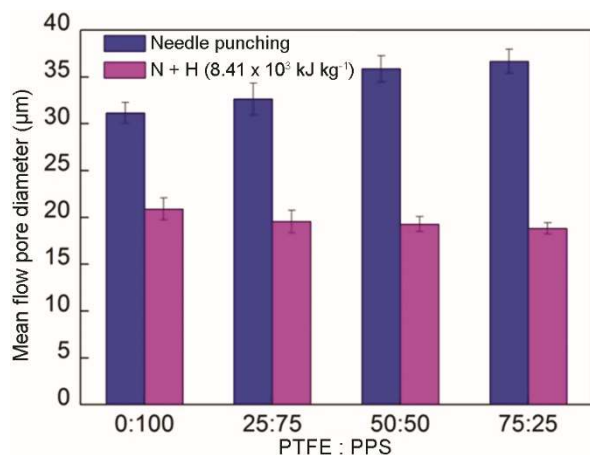


Fig. 6 — Relationship between mean pore size and blend ratio of hybrid fabric filters for needle punching and composite bonding process with specific energy of $8.41 \times 10^3$ kJ kg$^{-1}$

kinds of bonding processes, namely needle punching and needle punching + hydroentanglement with a fixed specific energy of $8.41 \times 10^3$ kJ kg$^{-1}$. The mean flow pore size of fabrics composed of same component decreases after being consolidated by hydroentanglement. This decrease seems to be statistically important and can be explained by the effective bonding of fibres occurred, and hence the distance between fibres becomes closer, resulting in a decreased mean pore size.

In addition, it could be inferred from Fig. 6 that for the fabrics composed of four different components, PTFE rich fabrics has largest mean pore size before hydroentanglement, whereas they possess lowest pore size after being subjected to the fluid forces. It has been reported that the formation of larger pore size is primarily due to the presence of coarser fibres[28]. As the diameter of PTFE fibres is larger than that of the PPS fibres, the mean pore size of the fabrics containing high proportion of PTFE is larger than that of PPS rich fabrics. However, after applying high-energy water jets, the average fibre diameter of PTFE becomes smaller than that of PPS, thus the PTFE rich fabrics own smaller mean pore size.

### 3.4 Effect of Blend Ratio on Filtraion Properties

Test apparatus (VDI 3926:2004) includes all the important operational parameters that a filters may encounter in baghouse using reversed pulse-jet of compressed air for periodically cleaning the filter. Table 4 shows the important parameters for fabric filters with different blend ratios of PPS and PTFE fibres consolidated by needle punching and composite bonding processes respectively. As compared to needle punched fabrics, the clean gas concentration becomes smaller after consolidated by hydroentanglement for all the component, indicating better filtration efficiency. Also they have smaller residual pressure drop with less residual dust mass, this could be attributied to the more compact structure, impeding the deposition or penetration of dust.

| Table 4 — Filtration properties for four different blend ratios of fabric filters | | | | | |
|---|---|---|---|---|---|
| Properties | Bonding process | Blend ratio (PTFE: PPS) | | | |
| | | 0:100 | 25:75 | 50:50 | 75:25 |
| Residual Pd, Pa | N | 675 | 692 | 721 | 754 |
| | N+H | 558 | 501 | 471 | 448 |
| Residual dust mass, g m$^{-2}$ | N | 185.8 | 192.4 | 212.4 | 232.5 |
| | N+H | 172.9 | 162.1 | 149.5 | 118.2 |
| Clean gas concentration, mg m$^{-3}$ | N | 0.75 | 0.83 | 0.94 | 1.12 |
| | N+H | 0.64 | 0.58 | 0.36 | 0.25 |

Table 4 shows that with the increase in PTFE proportion, the clean gas concentration decreases with less residual pressured drop and dust mass, when going through thousands of pulse-jet cleaning and clogging cycles. The reason could be attributed to the increased proportion of finer fibre diameter. The mean pore size decreases (Fig. 6), which makes it more difficult for the dust particles to be trapped or go through. As a result, the fabric filters composed of 75% PTFE with composite bonding process possess the superior filtration properties.

## 4 Conclusion

**4.1** As a result of SEM images and calculation, fibrillation could be observed for the fabric filters made of PTFE fibres when applied to the high-energy water jets. This indicates that the hydroentanglement could faciliate more obvious fibrillation of PTFE fibres as compared to needle punching process, and with the increase of specific energy the average fibre diameter of PTFE is decreased.

**4.2** Two–way ANOVA results show that the blend ratio and bonding process have significant effects on the air permeability, mean pore size and clean gas concentration.

**4.3** For fabrics composed of highest proportion of PTFE fibres, the air permeability and mean pore size are found to be the lowest after being consolidated by needle punching + hydroentanglement. However, they have the highest air permeability and mean pore size when consolidated only by needle punching. This can be attributed to the increased proportion of finer PTFE fibres owing to the fibrillation of PTFE fibres caused by high-energy water jets. With the increased proportion of PTFE fibres, the clean-gas concentration decreases, indicating better filtration efficiency.

## Acknowledgement

## References

1  Lin J H, Lou C W, Lei C H & Lin C Y, *Compos Part A*: *Appl Sci Manufac*, 37 (2006) 31.
2  Tanthapanichakoon W, Furuuchi M, Nitta K-h, Hata M, Endoh S & Otani Y, *Polym Degrad- Stabil*, 91 (2006) 1637.
3  Tanthapanichakoon W, Furuuchi, M, Nitta, K-h, Hata M & Otani Y, *Adv Powder Technol*, 18 (2007) 349.
4  Aleksandrov V P, Baranova R B & Valdberg A Y, *Chem Petrol Eng*, 46 (2010) 33.
5  Saleem M, Khan R U, Tahir M S & Krammer G, *Powder Technol*, 214 (2011) 388.
6  Rud H, Mauschitz G & Höflinger W, *J Hazard Mater*, 144 (2007) 742.
7  Mukhopadhyay A, *Text Prog*, 41 (2009) 195.
8  Zhang Q, Zhang S, Chen S, Li P, Qin T & Yuan S, *J Colloid Interface Sci*, 322 (2008) 421.
9  Lupión M, Gutiérrez O F J, Navarrete B & Cortés V J, *Fuel*, 89 (2010) 848.
10  Li M, Zhang W, Wang C & Wang H. *J Appl Polym Sci*, 123 (2012) 1667.
11  Borkar S, Gu B, Dirmyer M, Delicado R, Sen A, Jackson B R & Badding J V, *Polymer*, 47 (2006) 8337.
12  Zhang D N, Kou K C, Zhang Y, Zhao Q X & Zheng Z C, *J Appl Polym Sci*, 130 (2013) 3710.
13  Yeo S Y, Kim O S, Lim D Y, Byun S W & Jeong S H, *J Mater Sci*, 40 (2005) 5393.
14  Hoeflinger W, Rud H & Mauschitz G, *Sep Purif Technol*, 58 (2007) 256.
15  Pearce C E, DeLeon S, Putnam M, Carlson C & Hao P, *U S Pat* 7, 381, 669, June 2008.
16  Faulkner R, Hao P & Lindblom P, *U S Pat* 6,942,711, September 2005.
17  Lang A, *Che Fiber Int*, 56 (2006) 312.
18  Berkalp O B, *Fibres Text East Eur*, 14 (2006) 81.
19  Subramaniam V, Madhusoothanan M & Debnath C, *Text Res J*, 58 (1988) 677.
20  Liu Y, Cheng B, Wang N, Kang W, Zhang W, Xing Keqi & Yang W, *J Appl Polym Sci*, 124 (2012) 296.
21  Hoeflinger W, *Proceedings*, *4th Global Conference on Power Control & Optimazation PCO, Sarawak* (American Institute of Physics), 2010,1.
22  Wimmer A, *Filter Sep*, 36 (1999) 26.
23  Lawrence C & Liu P, *Chem Eng Tech*, 29 (2006) 957.
24  Hajiani F, Hosseini S, Ansari N & Jeddi A, *Fiber Polym*, 11 (2010) 798.
25  Payen J, Vroman P, Lewandowski M, Perwuelz A, Callé-Chazelet S & Thomas D, *Text Res J*, (2012) 1.
26  Atwal M S, *Text Res J*, 57 (1987) 574.
27  Russell S J, *Handbook of Nonwovens* (CRC Press Boca Raton), 2007, 266.
28  Rawal A & Saraswat H, *Geotext Geomembrane*, 29 (2011) 363.